Strain Relief Guided Growth of Atomic Nanowires in a Cu_3N-Cu(110) Molecular Network

X.-D. Ma,[1] D. I. Bazhanov,[1,2] O. Fruchart,[1,3] F. Yildiz,[1] T. Yokoyama,[4] M. Przybylski,[1,*] V. S. Stepanyuk,[1,†] W. Hergert,[5] and J. Kirschner[1]

[1]*Max-Planck-Institut für Mikrostrukturphysik, Weinberg 2, D-06120 Halle, Germany*
[2]*Moscow State University, GSP-1, Lenin Hills, 119991 Moscow, Russia*
[3]*Institut Néel, CNRS et Université Joseph Fourier, BP 166, F-38042 Grenoble Cedex 9, France*
[4]*Institute for Molecular Science, Myodaiji-cho, Okazaki, Aichi 444-8585, Japan*
[5]*Martin-Luther-Universität Halle-Wittenberg, Friedemann-Bach-Platz 6, D-06099 Halle, Germany*

(Received 6 January 2009; published 20 May 2009)

A self-corrugated Cu_3N-Cu(110) molecular network shows the potential to overcome the element dependence barrier as demonstrated by epitaxial growth of atomic nanowires (~1 nm in width) among various 3*d*, 4*d*, and 5*d* elements. Scanning tunneling microscopy shows that all of the investigated atomic nanowires share an identical structure, featuring uniform width, height, orientation and the same minimum separation distance. *Ab initio* study reveals that the formation mechanism of atomic nanowires can be directly attributed to a strain relief guided asymmetric occupation of atoms on the originally symmetric crest zone of the corrugated network.

DOI: 10.1103/PhysRevLett.102.205503 PACS numbers: 61.46.Km

Atomic nanowires are likely to play a vital role in future electronic devices built up at the nanometer scale [1]. As a cost effective method to prepare nanowires on an atomic scale, self-organization methods have drawn a lot of attention. Various self-organizing methods have been reported to prepare atomic nanowires: for instance, atomic chains prepared on metallic vicinal surfaces [2–4], linear arrays of nanostructures on vicinal Si surfaces [5], and many others.

A general phenomenon which has often been observed in self-organizing processes is the dependence of growth behavior on the combination of substrate and element. For example, on vicinal Pt(111), Co tends to form one dimensional atomic chains, while Ni does not due to substantial Pt-Ni intermixing [3]. On vicinal Cu(111) surfaces, Fe forms monoatomic chains while Co gives rise to nanoislands [4]. On flat Ge and Si(001) surfaces, it has been reported that 5*d* elements tend to form atomic chains while 4*d* elements do not [6]. Although the reason is still under debate, a plausible picture is that the strong relativistic character of the 5*d* electronic states lead to the formation of atomic nanowires [7].

In this Letter we report on the growth behavior of epitaxial atomic nanowires among a variety of 3*d*, 4*d*, and 5*d* elements on a corrugated molecular Cu_3N network on a Cu(110) surface. *Ab initio* calculations are employed to understand the formation principle of the atomic nanowires on the Cu_3N network. In particular, the strain relief guided occupation of atoms is discussed. Moreover, we have confirmed that the Cu_3N on a Cu(110) surface forms a polar covalently bonded molecular network with a band gap exceeding 3 eV, which is similar to the copper nitride on a Cu(001) surface [8].

The copper nitride Cu_3N network was prepared on a clean single crystalline Cu(110) surface [9–12]. N_2 was backfilled into the chamber at 1×10^{-7} mbar and activated by using an ion gun with a beam energy of 0.6 keV. The N^+ dosing density was kept at 2.4×10^{12} ions/cm^{2}s. The N^+ nitriding was performed at a temperature of around 700 K resulting in a fully reconstructed Cu_3N network with a terrace width of several hundred nanometers and completely free from N^+ sputtering damage. Based on the N^+ dosing density and the dosing duration, the coverage of N was calculated to be around 0.65 ML (1 ML $= 1.1 \times 10^{15}$ atoms/cm^2, which relates to the density of atoms on the Cu(110) surface).

Figure 1(a) shows a high-resolution scanning tunnelling microscopy (STM) image of the Cu_3N network: the distance between the two nearest bright features along the [001] direction is 11 Å and the distance between the two maximally bright features in each chain along the [1-10] direction is 5 Å. This structure demonstrates the Cu_3N network possessing $p(2 \times 3)$ periodicity, which is consistent with the low energy electron diffraction pattern (not shown). The Cu_3N network has corrugation with ~0.5 Å depth as shown in the line profile along xx' in Fig. 1(a). *Ab initio* calculations were carried out to examine the structural details concerning the corrugation of the Cu_3N network. We used molecular dynamics calculations based on density functional theory as it is implemented in the Vienna *ab initio* simulation package (VASP) [13]. VASP code was used to solve Kohn-Sham equations with periodic boundary conditions and a plane-wave basis set. For total energy and force calculations, we employed an all-electron projector augmented wave method [14]. The electron exchange and correlation effects have been taken into account using generalized gradient approximation [15]. We used a maximal kinetic energy cutoff of 400 eV which can converge iteratively on the total energy of the considered systems to within 1 meV/atom. The integration over the Brillouin zone has been performed using the well con-

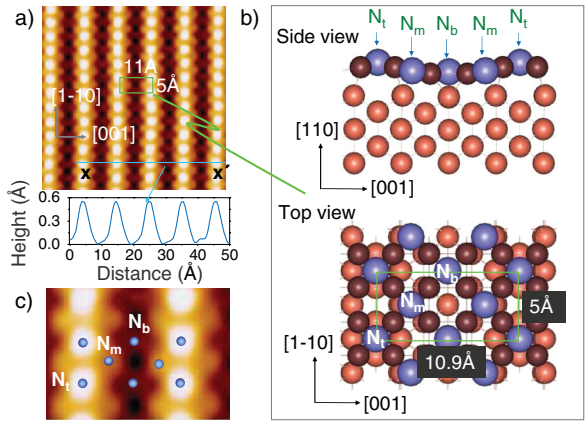

FIG. 1 (color). (a) High-resolution room temperature STM image (60 Å × 60 Å, 0.37 nA, 750 mV) with line profile along xx'. (b) Schematic view of the atomic structure for one corrugation unit on the Cu_3N network from *ab initio* calculations. N_t, N_m, and N_b represent the top, middle, and bottom positions, respectively, for N atoms. (c) STM image (14 Å × 20 Å) magnified from image (a), superimposed upon N atoms based on the structural model. Blue, dark brown, and light brown spheres denote N atoms including N_t, N_m, and N_b in the top layer of the Cu_3N, Cu atoms in the top layer of the Cu_3N, and Cu atoms below the Cu_3N network, respectively.

verged k meshes of $4 \times 4 \times 1$, $4 \times 6 \times 1$ and $4 \times 8 \times 1$ grids. Structural relaxations were determined via a quasi-Newton algorithm using the exact Hellmann-Feynman forces acting on each atom. The Monkhorst-Pack scheme [16] was used for k-point sampling of the Brillouin zone.

We explored two of the surface reconstruction models, which have been favored as the most reliable ones according to recent experimental structural studies: the so-called [110]-missing-row model [11] and the pseudo-(100) model [17]. The former model reproduces the $p(2 \times 3)$ surface nitride phase by removing each third row of Cu atoms along the [110] direction. We found that for nitrogen atoms, the subsurface so-called long bridge sites of a substrate are not favorable positions for bonding. They exhibit a strong upward relaxation and prefer to segregate towards the surface, infringing on a 0.66 ML nitrogen coverage requirement.

The pseudo-(100) model involves a formation of a surface nitride Cu_3N within the reconstructed surface layer of the Cu(110) substrate, consisting of a nearly square array of Cu atoms with a $c(2 \times 2)$ arrangement of N atoms [see Fig. 1(b), top view]. This surface nitride structure is similar to that observed for N chemisorption on Cu(001), where nitrogen atoms are adsorbed at the fourfold hollow sites, being nearly coplanar to the reconstructed surface layer [18]. We carried out first-principles calculations to study in detail the structural parameters of the surface nitride phase based on the proposed pseudo-(100) reconstruction model. The obtained results demonstrate that the $p(2 \times 3)$ Cu_3N nitride surface phase, represented by a pseudo-(100) surface reconstruction model, exhibits a large expansion of interlayer spacing (about +53%) between surface reconstructed and subsurface unreconstructed copper layers. The corrugation amplitude of the Cu_3N network along the [001] direction is about 0.5 Å, which is consistent with the value measured by STM. As shown in Fig. 1(b), the corrugation of the surface layer results in two raised and two lowered rows of copper atoms with a strong displacement from their original position on the clean Cu(110) surface. Nitrogen atoms form a regular $c(2 \times 2)$ atomic structure by their adsorption at three different hollow sites (designated as N_t, N_m, and N_b,—on the top, middle and at the bottom, respectively) within a one trough distance of the corrugated surface copper nitride layer [see Fig. 1(c)]. Our calculations indicate that Cu and N atoms within the Cu_3N layer are covalently polar bonded yielding a similar molecular network as reported on Cu(100) [8]. The pseudo-(100) surface is rigorously verified by the atomic resolution STM image shown in Fig. 1(c), where the positions of N_t, N_m and N_b atoms are superimposed onto the corresponding *ab initio* model. The middle N atoms (N_m) are better resolved at the place where the top N atoms, i.e., N_t are missed.

Such a Cu_3N network allows a growth of atomic nanowires. All of the nanowires shown in Figs. 2(a)–2(d) were deposited on the Cu_3N network at room temperature by molecular beam epitaxy (MBE). Nanowires made of different elements show an identical structure. We give a detailed description by taking the Fe atomic nanowire as a representative example. Figure 2(a) shows 0.05 ML of Fe on a Cu_3N network prepared by MBE at a growth rate of 0.2 ML/ min. The line profile of a single Fe nanowire in Fig. 2(a) shows that the height of the wire is ~1.23 Å. The width at FWHM of the wire is found to be 11 Å, which is verified later by atomic resolution STM of the nanowire, see Fig. 3(c). As shown in Fig. 1(b), the calculated width of one trough of the corrugated Cu_3N network is 10.9 Å. This

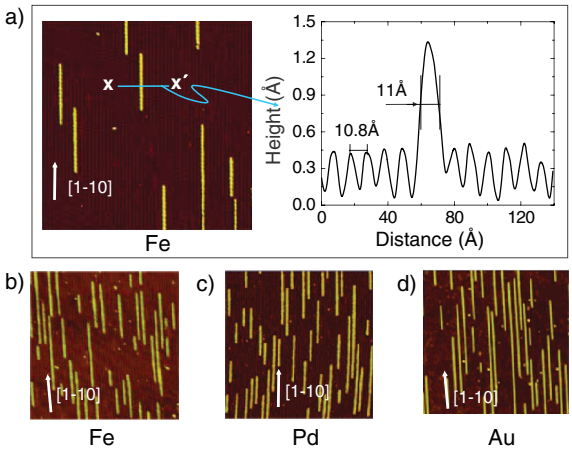

FIG. 2 (color). (a) STM image (570 Å × 570 Å, 0.45 nA, 860 mV) of atomic nanowires after deposition of 0.05 ML of Fe and the line profile along xx'. (b),(c) and (d) show STM images of atomic nanowires after deposition of 0.2 ML of Fe, Pd, and Au, respectively (all three STM images are sized 700 Å × 700 Å).

indicates that each individual atomic nanowire occupies a single trough of the Cu_3N network. No width distribution is found for the grown atomic nanowires. An identical structure of atomic nanowires made of different elements on the Cu_3N network is confirmed in Figs. 2(b)–2(d) where atomic nanowires with coverage of 0.2 ML Fe, 0.2 ML Pd, and 0.2 ML Au are presented. It is also seen that the Fe nanowires at the coverage of 0.05 and 0.2 ML of Fe are identical. The same nanowire structures for other elements such as Mn, Ni, Rh, Cr, Co are not shown here due to limited space.

A combined high-resolution STM study and *ab initio* calculations were performed to clarify the atomic structure of individual atomic nanowires on the Cu_3N-Cu(110). Based on the surface nitride $p(2 \times 3)$ structure of the Cu_3N network, we studied the binding properties of the most coordinated adsorption sites with regard to the Cu_3N surface plane. Owing to the corrugation of the $p(2 \times 3)$ Cu_3N nitride phase, there are three different fourfold hollow sites [designated in Fig. 3(a) as 1, 3, and 5, for top, intermediate and bottom Fe atoms, respectively], and two different threefold bridge sites (designated as 2 and 4 for top and bottom Fe atoms) for adsorption within the $p(2 \times 3)$ unit cell. To simulate Fe nanowires we used a supercell approach. The supercell structure consists of a 6 atomic layer slab of Cu(110) substrate with N atoms embedded into the upper surface layer and Fe atoms deposited on top of the Cu_3N surface network. The vacuum region between repeated slabs is 10 Å. For all calculations, the two bottom layers of the slab have a fixed interlayer distance of 1.28 Å (which refers to the distance between the nearest crystalline planes along [110] direction for bulk Cu), while other atomic layers are relaxed until the forces are converged in the supercell. The calculations for adsorbed Fe adatoms on $p(2 \times 3)$ Cu_3N indicate that the bridge sites (2 and 4) are energetically less favorable than the hollow sites (1, 3, and 5). We observe that adsorption of a Fe adatom at the bridge site causes a substantial vertical displacement of the Cu atom directly below this adatom. This Cu atom exhibits a strong relaxation towards the Cu bulk and will no longer be a part of the surface nitride phase. Fe adatoms have a high adhesion at the hollow sites surrounded by copper atoms of the Cu_3N network, where the most favorable binding site is at the bottom of the trough (site 5). With respect to site 5, the sites 1 and 3 have an energy loss of 1.36 eV and 1.85 eV, respectively.

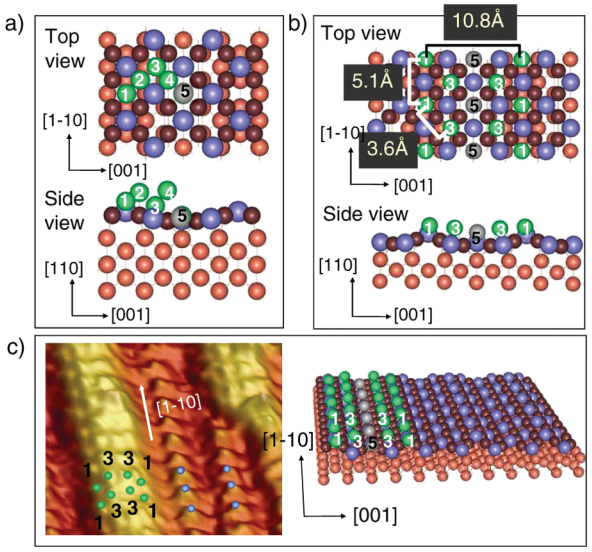

FIG. 3 (color). (a) The top view shows three different fourfold hollow sites of the Cu_3N network which are designated as 1, 3, and 5, for the top, intermediate, and bottom Fe atoms, respectively, and two different threefold bridge sites 2 and 4, for top and bottom Fe atoms. The side view shows that the positions of the Fe adatoms at sites 2 and 4, according to the results of *ab initio* calculation, are higher than the ones at other sites. (b) Schematic view of the atomic structure of a single Fe nanowire from *ab initio* calculations. Each nanowire is five atomic rows in width. Fe atoms at the top (1), intermediate (3) and bottom (5) adsorption sites are shown in side view. (c) STM image of the Fe atomic nanowire (39 Å × 48 Å, 0.46 nA, 500 mV) superimposed upon the Fe atom positions from *ab initio* study. The structural model is placed to the right for better understanding. In (a), (b), and (c); blue, dark brown, light brown, and light green colors denote all N atoms in the top layer of the Cu_3N, Cu atoms in the top layer of the Cu_3N, Cu atoms below Cu_3N network, and Fe atoms, respectively. Note: The bottom Fe atoms (5) are shown in gray color since they are deeply embedded into the Cu_3N network and hence hardly visible in the STM image.

We next studied the formation process and structural parameters of the Fe atomic wires on the Cu_3N network. Based on structural information obtained by STM, we examined each Fe atomic wire consisting of individual atomic rows running along the [110] direction and occupying a relatively stable hollow site, one belonging to a single trough of the corrugated Cu_3N network [see Fig. 3(b)]. In addition, from Fig. 3(b) one can see that each nanowire consists of five atomic rows with Fe atoms at the top (1), intermediate (3), and bottom (5) adsorption sites of the trough. The nanowires have a width of 10.8 Å, slightly less than the width of a trough (10.9 Å), due to attractive interatomic interaction between Fe atoms trying to enhance their bonding at the surface. The theoretical value of this width coincides remarkably well with the experimental value (11.0 Å) measured with STM. It is seen in Fig. 3(b) that the Fe atoms are arranged in individual rows, in a zigzag order within the nanowire, with an average bond length of 3.6 Å in inter-row spacing and with a bond length of 5.1 Å along the rows. The obtained spacing is consistent with the geometry of the fcc(110) surface observed on the Cu_3N network. The agreement between theory and experiment is further confirmed by the positions of Fe atoms shown in Fig. 3(c), where a model of a single atomic wire from *ab initio* study and an atomically resolved STM image are presented. It should be noted here that the relaxation of Fe row (5) adsorbed in the bottom of the trough results in the least height (1.42 Å) above the nearest copper atoms of the surface nitride layer with

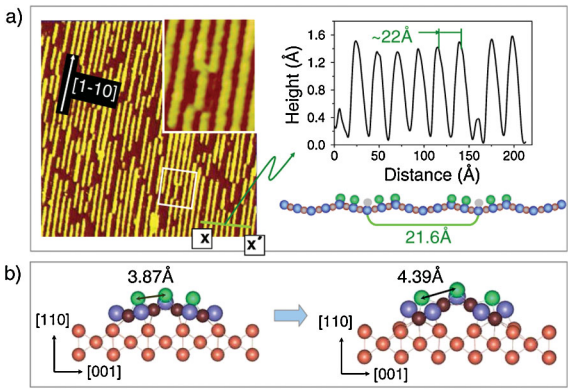

FIG. 4 (color). (a) STM image (700 Å × 700 Å, 0.5 nA, 860 mV) of Fe atomic nanowires at coverage of 0.4 ML with line profile (right side) along xx'. The inset magnified image clearly shows that the occupation at the trough nearest to the atomic nanowire is strictly forbidden. The structural model below the line profile is shown to demonstrate the existence of a minimum separation distance. (b) The left and right figures show the structure obtained from *ab initio* studies before and after relaxation. Atoms on the crest region become unstable due to the increased Fe-Fe bond distance once both sides of the crest are symmetrically occupied. Here, colors of the atoms are exactly the same as in Fig. 3.

respect to the other Fe rows. This result explains the absence of bright spots ascribed to the bottom Fe atoms (5) in the middle of the Fe wire, seemingly resulting in the four atomic rows observed by STM, as it is shown in Fig. 3(c).

As shown in Fig. 4(a), from the line profile and the structural model below it we found a minimum distance of 21.6 Å between the nanowires, which corresponds exactly to the double periodicity (×6) of the Cu_3N-(2 × 3) network along the [001] direction. This double periodicity can also be seen in the inset magnified image in Fig. 4(a), which clearly shows that occupation of the trough nearest to the atomic nanowire is strictly forbidden. This means that a symmetrical occupation on both sides of the crest region between the two nearest troughs may be thermodynamically and kinetically unfavorable. We performed calculations for Fe rows deposited on the crest region of a $p(2 \times 3)$ Cu_3N network (one row on top and another two ones at intermediate positions) in order to examine the bonding properties at these positions [see Fig. 4(b), left]. The calculated results show that N atoms in the crest region shift into deposited Fe rows due to their strong covalent bonding with Fe atoms. Formation of Fe-N bonds leads to a large tensile strain propagating across the whole crest region and significantly increases the inter-row spacing of Fe atoms, up to 4.39 Å, as shown in Fig. 4(b) (right). Thus, the bond between the Fe rows becomes weak due to bonding competition between Fe-Fe bonds and Fe-N bonds which makes the symmetric occupation on both sides of the crest region thermodynamically unstable. As a consequence, the occupation of Fe atoms becomes asymmetric and only one side of the crest region can be occupied due to the strain relief. Moreover, *ab initio* study has confirmed an observation that within a single trough, five atomic rows of adsorption always lead to the lowest total energy of the system among all of the nanowires with fewer rows. The asymmetric occupation that originated from the intrinsic corrugation nature of the Cu_3N network indicates that this formation principle can be valid for the other elements, pointing towards the existence of a universal growth behavior on the Cu_3N network.

In summary, we have observed an identical growth behavior of epitaxial atomic nanowires made of different elements on a self-corrugated molecular Cu_3N network prepared on a single crystalline Cu(110) surface. All of the atomic nanowires possess an identical structure characterized by uniform width, height and orientation, as well as exhibiting a minimum separation distance corresponding to double periodicity of the Cu_3N network along the [001] direction. *Ab initio* calculations reveal that the common formation principle for these atomic nanowires can be attributed to the strain relief guided asymmetric occupation of atoms at the crest region of the Cu_3N network.

We thank H. Menge and G. Kroder for technical support. V. S. S. and W. H. acknowledge financial support from SPP-1165 project.

*mprzybyl@mpi-halle.mpg.de
†stepanyu@mpi-halle.mpg.de

[1] W. Yue, J. Xiang, C. Yang, W. Lu, and C. M. Lieber, Nature (London) **430**, 61 (2004).
[2] S. Shiraki, H. Fujisawa, M. Nantoh, and M. Kawai, Appl. Surf. Sci. **237**, 284 (2004).
[3] P. Gambardella and K. Kern, Surf. Sci. **475**, L229 (2001).
[4] J. D. Guo, Y. Mo, E. Kaxiras, Z. Zhang, and H. H. Weitering, Phys. Rev. B **73**, 193405 (2006).
[5] T. Sekiguchi, S. Yoshida, and K. Itoh, Phys. Rev. Lett. **95**, 106101 (2005).
[6] J. Wang, M. Li, and E. I. Altman, Phys. Rev. B **70**, 233312 (2004).
[7] A. A. Stekolnikov, F. Bechstedt, M. Wisniewski, J. Schfer, and R. Claessen, Phys. Rev. Lett. **100**, 196101 (2008).
[8] C. F. Hirjibehedin *et al.*, Science **317**, 1199 (2007).
[9] D. Heskett, A. Baddorf, and E. W. Plummer, Surf. Sci. **195**, 94 (1988).
[10] A. P. Baddorf, Phys. Rev. B **48**, 9013 (1993), and references therein.
[11] F. M. Leibsle, R. Davis, and A. W. Robinson, Phys. Rev. B **49**, 8290 (1994).
[12] S. M. York and F. M. Leibsle, Phys. Rev. B **64**, 033411 (2001).
[13] G. Kresse and J. Hafner, Phys. Rev. B **48**, 13 115 (1993).
[14] G. Kresse and J. Furthmuller, Comput. Mater. Sci. **6**, 15 (1996).
[15] G. Kresse and D. Joubert, Phys. Rev. B **59**, 1758 (1999).
[16] P. E. Blochl, Phys. Rev. B **50**, 17 953 (1994).
[17] H. Wende, D. Arvanitis, M. Tischer, R. Chauvistre, H. Henneken, F. May, and K. Baberschke, Phys. Rev. B **54**, 5920 (1996).
[18] F. M. Leibsle, Surf. Sci. **514**, 33 (2002).